



HAL
open science

Boson-Fermion Duality and Metastability in Cuprate Superconductors

Julius Ranninger, T. Domanski

► **To cite this version:**

Julius Ranninger, T. Domanski. Boson-Fermion Duality and Metastability in Cuprate Superconductors. *Physical Review B: Condensed Matter and Materials Physics (1998-2015)*, 2010, pp.014514. 10.1103/PhysRevB.81.014514 . hal-00717404

HAL Id: hal-00717404

<https://hal.science/hal-00717404>

Submitted on 16 Feb 2022

HAL is a multi-disciplinary open access archive for the deposit and dissemination of scientific research documents, whether they are published or not. The documents may come from teaching and research institutions in France or abroad, or from public or private research centers.

L'archive ouverte pluridisciplinaire **HAL**, est destinée au dépôt et à la diffusion de documents scientifiques de niveau recherche, publiés ou non, émanant des établissements d'enseignement et de recherche français ou étrangers, des laboratoires publics ou privés.

Boson-Fermion Duality and Metastability in Cuprate Superconductors

J. Ranninger¹ and T. Domański²

¹*Institut Néel, CNRS et Université Joseph Fourier, BP 166, 38042 Grenoble Cedex 09, France*

²*Institute of Physics, Marie Curie-Skłodowska University, 20-031 Lublin, Poland*

(Dated: November 3, 2018)

The intrinsic structural metastability in cuprate high T_c materials, evidenced in a checker-board domain structure of the CuO_2 planes, locally breaks translational and rotational symmetry. Dynamical charge - deformation fluctuations of such nano-size unidirectional domains, involving Cu-O-Cu molecular bonds, result in resonantly fluctuating diamagnetic pairs embedded in a correlated Fermi liquid. As a consequence, the single-particle spectral properties acquire simultaneously (i) fermionic low energy Bogoliubov branches for propagating Cooper pairs and (ii) bosonic localized glassy structures for tightly bound states of them at high energies. The partial localization of the single-particle excitations results in a fractionation of the Fermi surface as the strength of the exchange coupling between itinerant fermions and partially localized fermion pairs increases upon moving from the nodal to the anti-nodal point. This is also the reason why, upon hole doping, bound fermion pairs predominantly accumulate near the anti-nodal points and ultimately condense in an anisotropic fashion, tracking the gap in the single particle spectrum.

PACS numbers: 74.20.-z, 74.20.Mn, 74.40.+k

I. INTRODUCTION.

High T_c superconductivity of the cuprates, it is generally agreed upon, emerges out of an unconventional normal state. The most remarkable signatures of its strange metal behavior are the pseudogap in the density of states and the associated to it remnant Bogoliubov modes. Both show up in a wide temperature regime above T_c in the single-particle excitations, observed in angle resolved photoemission spectroscopy (ARPES)¹. Novel scanning tunneling microscopy are now able to measure the spatial distribution of quasi-particle excitations on the atomic length scale²⁻⁶ and find intrinsic textured electronic structures, ranging over a wide regime from low doped to optimally doped and beyond. The spatial patterns of the single-particle spectral properties indicate an inter-relation between the low frequency Bogoliubov modes and their high frequency counterparts, representing localized glassy structures. In this work we show how this feature can be related to a scenario in which itinerant fermionic charge carriers scatter in and out of bosonic tightly bound pairs of them in which they are momentarily trapped on nano-size deformable molecular clusters. The single-particle excitations thus appear as superpositions of itinerant and localized entities. Ever since the discovery of the high T_c cuprates, experimental evidence for their very unusual lattice properties has become increasingly evident. Apart from their well established strongly correlated nature, these compounds are metastable single phase materials⁷. Their metastability arises from frozen-in structural misfits, involving an incompatibility between the Cu-O distances of square planar $[\text{Cu-O}_4]$ configurations in the CuO_2 planes and of cation-ligand distances in the adjacent layers. Metastable compounds have been known for a long time for their intrinsic local diamagnetic fluctuations⁸, capable of inducing a strong pairing component in the many-body ground

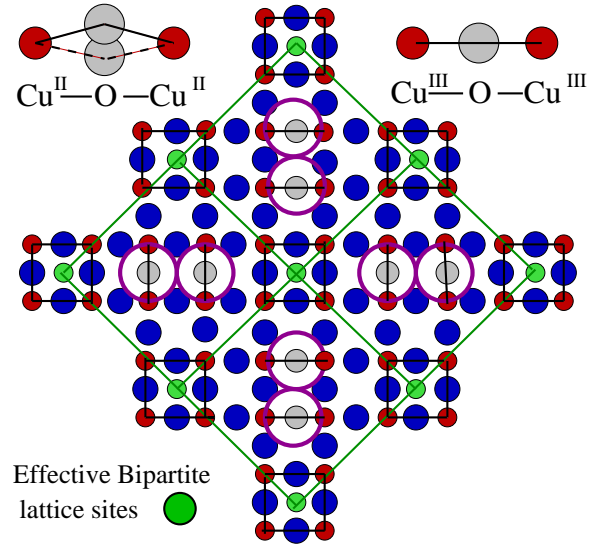


FIG. 1: (Color online) An idealized picture of the local structure of the CuO_2 planes, compatible with the STM results²⁻⁶. It is composed of (i) Cu_4O_{12} domains acting as localizing pairing centers with directionally oriented Cu-O-Cu molecular bonds, having central bridging O's (grey circles) which can be displaced out of the CuO_2 plane and (ii) Cu_4O_4 square plaquettes housing the delocalized charge carriers. Small red circles denote Cu cations and the larger blue ones the O anions not directly involved in displacements.

state wave function. The interest in synthesizing materials with such properties was to bypass the stringent conditions on the upper limit of T_c , imposed by phonon mediated BCS superconductivity⁹.

On a microscopic level, the metastability in the cuprates arises from fluctuating $[\text{Cu-O-Cu}]$ molecular bonds in the CuO_2 planes^{2,3}. Their deformable lig-

and environments^{10,11} act as potential pairing centers⁴ induced in the undoped systems upon hole doping. These nano size domains exhibit an atomic structure⁵, which locally breaks translational as well as rotational symmetry⁶. Two degenerate spatially orthogonally oriented [Cu-O-Cu] bonds cause the CuO₂ plane structure to segregate into a patchwork of orientationally disordered domains, separated by a lattice of essentially undeformable molecular clusters. Ultimately, this forms an effective bipartite lattice structure^{2,6} of the CuO₂ planes. The charge transfer between the pairing centers and the molecular clusters on the lattice surrounding them leads to resonant pairing on that latter. It is controlled by an interplay between localization of the charge carriers in form of bound pairs on the pairing centers and their delocalization on the lattice which spatially separates them. On a macroscopic level, those materials exhibit an overall homogeneous crystal structure in a coarse grained sense¹². But occasionally, such as in La_{2-x}Ba_xCuO₄ for x=1/8, the local lattice deformations of the pairing centers lock together in a charge ordered phase and thereby impeach superconductivity to occur⁵.

II. THE SCENARIO

The "formal chemical" Cu valence - not to be confused with its ionic charge - in the d-hole doped CuO₂ planes lies between Cu^{II} and Cu^{III}. For an isolated undoped CuO₂ plane this would correspond to stereochemical [Cu^{II}-O] distances of 1.94 Å in the [Cu-O₄] basic blocks. The misfits between the atomic structure of the CuO₂ planes and those of the adjacent layers, which furnish the dopant holes, push the bridging oxygen of the [Cu-O-Cu] bonds out of the CuO₂ plane, making them buckled. By doing so, they can accommodate the stereochemically assigned inter-atomic distance of those bonds.

The scenario for the doped cuprates, which we want to advocate in this work, is that the static displacements of the bridging oxygens, which characterize the undoped and low doped insulating phase, become dynamic. The fluctuation of the bridging oxygens of the [Cu-O-Cu] bonds, in and out of the planes, tends to diminish the plane buckling which characterizes the undoped material. This tendency gets more and more pronounced as the doping is increased, driven by the increased covalency of the CuO₂ basal plane building blocks. It however shows a marked slowing down of this behavior as one passes through optimal doping¹³. On a microscopic level, this implies fluctuations between kinked [Cu^{II} - O - Cu^{II}] molecular bonds (characteristic for the undoped systems) and straightened out ones [Cu^{III} - O - Cu^{III}], with an ideal stereochemical [Cu^{III}-O] distances of 1.84 Å. In this process two electrons get momentarily captured in the local dynamically deformable structure of the CuO₂ planes. It results in locally correlated charge-deformation fluctuations which break up the over-all homogeneous structure of the cuprates into a checker-board

structure, as scanning tunneling microscopy (STM) results (Figs. 4 and 5 in Ref. 6) have shown. The net difference in length between the two different molecular bonds on such charge-deformation fluctuating checker-board pairing domains can be reduced (i) because of the dynamical nature of these pairing fluctuations and (ii) because it involves cooperatively several of such [Cu-O-Cu] bonds.

The likelihood of a segregation of a homogeneous lattice structure into polaronic domains, embedded in a non-polaronic matrix, such as advocated in the present scenario, had been speculated upon for a long time. For the case of intermediate electron-lattice coupling and the adiabatic to anti-adiabatic cross-over regime, individual itinerant charge carriers are known to fluctuate in and out of localized polaronic states¹⁴. Unfortunately, the present state of art of the theory of many-polaronic systems can still not handle situations other than for homogeneous or globally symmetry broken solutions. Nevertheless indications for resonant pairing in such systems exist, where the single-particle spectral function has both coherent delocalized contributions and localized ones in form of localized polarons, respectively bipolarons. This has been discussed in the framework of dynamical mean field theory, numerical renormalization group and Monte Carlo studies¹⁵.

Given the complexity of the inter-related charge-deformation dynamics in such systems, it appeared judicious to introduce a phenomenological Boson-Fermion model (BFM), to capture the salient features of such intrinsically locally dynamically unstable systems with a tendency to segregate into subsystems of localized and itinerant charge carriers. This idea was originally proposed by one of us (JR) in the early eighties in an attempt to describe the abrupt cross-over between a weak coupling adiabatic electron-phonon mediated BCS superconductor and an insulating state, respectively superconducting phase, of bipolarons in the strong coupling anti-adiabatic regime. The essential features of this conjectured BFM was to introduce an effective local boson-fermion exchange coupling between polaronically bound pairs and itinerant charge carriers. This picture has been substantiated subsequently by small cluster calculations for electrons strongly coupled to localized lattice vibrational modes¹⁶. It permits to relate the effective boson-fermion exchange coupling back to the parameters, characterizing the electron-lattice coupled system, ie., local phonon frequency and electron-phonon coupling.

In order to cast into a tractable model the physics of dynamically fluctuating [Cu-O-Cu] bonds, which trigger local double charge fluctuations, we present in Fig. 1 an idealized structure for such a local checker-board bipartite lattice structure, which comes very close to the actually observed structure. The corresponding checker-board pairing centers consist of Cu₄O₁₂ domains (three nearest neighbor Cu-Cu distances across) on which charge carriers pair up, driven by polaronic effects. The lattice deformations of adjacent Cu₄O₁₂ domains are as-

sumed to be uncorrelated in order to prevent the system to undergo a global lattice instability. The orientational randomness of the [Cu-O-Cu] unidirectional bonds, together with the quadratic Cu_4O_4 plaquettes (see Fig.1), which separate those polaronic Cu_4O_{12} domains, justifies that. Ultimately, this results in the picture of an overall bipartite lattice structure for the CuO_2 planes with a periodicity of four nearest neighbor Cu-Cu distances. d-holes on the non-polaronic Cu_4O_4 plaquettes in the cuprates are known to behave as delocalized, though strongly correlated, entities subject to $d_{x^2-y^2}$ - wave pairing correlations^{17,18}. In the present study we shall concentrate on the purely lattice driven pairing aspects in the cuprates, caused by their intrinsic metastabilities. We hence neglect here any Hubbard type correlations leading to hole pairing and treat the Cu_4O_4 square plaquettes as effective lattice sites on which the charge carriers behave as itinerant uncorrelated quasiparticles. When they hop on and off the Cu_4O_{12} pairing centers, they interact with their local dynamical deformations. The resulting local physics for resonant pairing for such a set-up and its manifestations in the electronic and phononic spectral properties have been studied in some detail by exact diagonalization studies¹⁶.

Indications for resonant pairing in the cuprates, driven by local dynamical lattice fluctuations can be found in quite a variety of experimental studies: the longitudinal optical (LO) Cu-O bond stretching mode of about 60 meV appears strongly coupled to charge carriers near the *hotspot* anti-nodal points in the Brillouin zone (BZ) $[q_x, q_y] = [\pm\pi/2, 0], [0, \pm\pi/2]$ ^{10,11}. Their pairing results in the pseudogap feature, setting in when reducing the temperature T to below a certain, strongly doping dependent, T^* . Upon entering the superconducting doping regime, coming from the insulating parent compound, this LO mode splits into two modes, separated by $\simeq 10$ meV¹⁹. This indicates a crystal lattice symmetry breaking, linked to dynamical charge inhomogeneities which are absent in the underdoped and overdoped insulating phases. Pressure²⁰, isotope substitution studies²¹ and atomic resolution d^2I/dV^2 -spectroscopy¹¹ show concomitant anticorrelated modulations of the pseudo-gap size and the frequency of this LO buckling mode. Correlated charge-deformation fluctuations, related to a resonant pairing superconducting phase show up in the onset of a macroscopic superfluid state of the charge carriers together with changes in the local lattice dynamics which acquires phase correlated macroscopic features. They are seen in Rutherford back scattering experiments²², an abrupt decrease in the kinetic energy of local vibrational modes²³, a similar abrupt increase of a low energy electronic background, seen in near IR excited Raman scattering²⁴ and an increase in intensity of certain Raman active phonon modes²⁵, indicative of changes in the scattering mechanism involving the charge carriers and local lattice modes.

III. THE MODEL

Superconductivity in the cuprates is destroyed, exclusively, by phase fluctuations of a bosonic order parameter^{26,27}, with the finite amplitude of it, being already established well above T_c . It reflects the local nature of the Cooper-pairs, whose signature is (i) a T_c scaling with the zero temperature density of superfluid carriers²⁸ and (ii) the XY character of the transition²⁹. Going into the normal state, above T_c , the propagating Cooperons become diffusive and the superconducting gap changes into a pseudogap in a continuous fashion³⁰. The observed Nernst³¹, transient Meissner effect³² and the proximity induced pseudogap³³ bare this out. The gap in the single-particle spectrum and the diffusively propagating strongly bound Cooper pairs testify the competition between amplitude and phase fluctuations of the order parameter in form of an anti-correlated T_c versus T^* variation upon changing the hole doping^{34,35}. The insulating, not antiferromagnetically ordered glassy state, at low temperature and low doping can be envisaged as a Mott correlation driven state of phase uncorrelated singlet-*bonding pairs*. With increased doping, this insulating state changes into a superconducting phase correlated state of such *bonding pairs*^{36,37}. *Bonding pairs* are defined by local linear superpositions of bound pairs and pairs of itinerant charge carriers. To what extent such an insulating state could result from a Cooper-pair Wigner crystallization, has been investigated^{38,39}.

The features which characterize the normal and superconducting phase of the cuprates necessitate to treat amplitude and phase fluctuations on an equal footing. This had originally also been the objective in conjecturing the BFM and to project out coexisting effective bosonic and fermionic charge excitations for systems which are at the frontier between amplitude fluctuation driven BCS superconductors and a phase fluctuation driven superfluidity of tightly bound real-space pairs. The BFM is designed to treat a single component system, where at any given moment a certain percentage of the charge carriers is locally paired and thus results in a finite bosonic amplitude. This is achieved by imposing a common chemical potential (determined by the bosonic energy level) for the fermionic and bosonic charge carriers. A charge exchange term, linking the fermionic and bosonic subsystem, then controls the inter-related dynamics between amplitude and phase fluctuations. It drives the system either to an insulating or superfluid state with corresponding superconducting, respectively insulating, gaps being centered at the chemical potential. The opening of such gaps does not depend on any particular set of Fermi wavevectors and hence is unrelated to any global translational symmetry breaking.

The degree of anisotropy of pairing and of the charge carrier dispersion in the CuO_2 planes monitors the relative importance of localization versus delocalization in different regions of the Brillouin zone. Near the anti-nodal points, strong pairing results from strong intra-

bonding pair correlations between bound pairs on the pairing centers and their itinerant counterparts in their immediate vicinity¹⁶. It leads to their partial localization, which shows up in form of a pseudogap in the single-particle spectral properties and destroys the Fermi surface. As one moves toward the nodal points, $[k_x, k_y] = [\pm\pi/2, \pm\pi/2]$, along the so-called Fermi arc in the Brillouin zone (corresponding to the Fermi surface in the non-interacting system), those intra-*bonding pair* phase correlations are weakened. The degree of localization then reduces and with it, the size of the pseudogap. At the same time, inter-*bonding pair* phase correlations between neighboring pairing domains come into play and with it, superconducting phase locking. At low energies, this leads to Bogoliubov like modes, which emerge out of localized phase uncorrelated *bonding pairs*. We derive below these properties on the basis of the BFM, adapted to the specific anisotropic features of the cuprates.

Transposing our picture of the cuprate molecular structure (Fig. 1) onto the BFM (see also Figs. 3 and 4 in Ref.⁴⁰) implies the following: We introduce effective lattice sites, which are composed of two components: One which represents the pairing centers (the Cu_4O_{12} domains) and describes selftrapped bosonic pairs of charge carriers. The other one which describes the itinerant charge carriers on the four-site ring, constituted of the Cu_4O_4 plaquettes, taking into account that each such plaquette is shared by four neighboring pairing centers. For the undoped half-filled band situation, with one electron per Cu site, we thus have four itinerant electrons on the ring, belonging to a specific pairing center and four electrons being localized in form of two $\text{Cu}^{II}\text{-O-Cu}^{II}$ bonds on the pairing centers. Deviating from the undoped limit upon doping n_h holes per Cu ion into the systems, reduces the concentration of $\text{Cu}^{II}\text{-O-Cu}^{II}$ bonds in the trapping centers by $n_B \simeq \frac{1}{2} n_h$. This opens up the phase space for itinerant electrons from the four-site ring to hop on off those trapping centers. Such a resonant scattering process converts a small number n_B of those itinerant charge carriers into bosonic bound pairs. Following the experimental results of the strong changes in local lattice properties with hole doping, we assume that hole doping monitors exclusively the concentration of the $\text{Cu}^{II}\text{-O-Cu}^{II}$ bonds and that hence the total number of itinerant electrons and induced pairs of them will remain roughly the same as it was in the undoped case, i.e., $n_{tot} = n_F + 2n_B = 1$.

The d-wave pairing symmetry of those systems imposes an analogous d-wave symmetry for the exchange interaction between (i) pairs of itinerant charge carriers $c_{\mathbf{k}\sigma}^{(\dagger)}$, corresponding to the "plaquette site" states and (ii) polaronically bound pairs of them $b_{\mathbf{q}}^{(\dagger)}$, corresponding to the "pairing center site" states. The Hamiltonian describing

such a scenario is then given by

$$H_{BFM} = H_{BFM}^0 + H_{BFM}^{exch} \quad (1)$$

$$H_{BFM}^0 = \sum_{\mathbf{k}\sigma} (\varepsilon_{\mathbf{k}} - \mu) c_{\mathbf{k}\sigma}^\dagger c_{\mathbf{k}\sigma} + \sum_{\mathbf{q}} (E_{\mathbf{q}} - 2\mu) b_{\mathbf{q}}^\dagger b_{\mathbf{q}}. \quad (2)$$

$$H_{BFM}^{exch} = (1/\sqrt{N}) \sum_{\mathbf{k}, \mathbf{q}} (g_{\mathbf{k}, \mathbf{q}} b_{\mathbf{q}}^\dagger c_{\mathbf{q}-\mathbf{k}, \downarrow} c_{\mathbf{k}, \uparrow} + H.c.), \quad (3)$$

The anisotropy, which characterizes the electronic structure of cuprates, is contained in the standard expression for the bare charge carrier dispersion given by $\varepsilon_{\mathbf{k}} = -2t[\cos k_x + \cos k_y] + 4t'\cos k_x \cos k_y$ of the CuO_2 planes with $t'/t = 0.4$ and the bare d-wave exchange coupling $g_{\mathbf{k}, \mathbf{q}} = g[\cos k_x - \cos k_y]$. Given the polaronic origin of the localized pairs of tightly bound charge carriers, we assume them as dispersionless bosonic excitations with $E_{\mathbf{q}} = 2\Delta$.

The charge exchange term H_{BFM}^{exch} controls the transfer of electrons (holes) between real and momentum space⁴¹ and monitors the interplay between the delocalizing and the localizing effect. Depending on the strength of the exchange coupling $g_{\mathbf{k}, \mathbf{q}}$, it results in a competition between local intra-*bonding pair* correlations, favoring insulating features, and spatial inter-*bonding pair* correlations, favoring superconducting phase locking³⁶. The fermionic particles thereby acquire contributions coming from the bosonic particles and the bosonic particles having features derived from their fermionic constituents. As we shall see below, the physically meaningful fermions in such a system are superpositions of fermions and bosonic bound fermion pairs, accompanied by fermion holes. This boson-fermion duality, which characterizes the electronic state of the cuprates, results from the "duplicitous"⁴¹ nature of their charge carriers, which supports simultaneously superconducting correlations in momentum space (fermionic Bogoliubov excitations) and real space correlations resulting in the pseudogap (derived from localized bosonic bound fermion pairs). This apparent "schizophrenic" behavior⁴² of the quasi-particles can be traced back to their different energy scales characterizing their excitations. Large excitation energies (above the Fermi energy) characterize their localized selftrapped nature and small excitation energies (below the Fermi energy) their quasi-coherently propagating Cooper pair nature.

In order to obtain the spectroscopic features of effective fermionic and bosonic excitations we have to reformulate this interacting Boson-Fermion mixture in terms of two effective commuting Hamiltonians, one describing purely fermionic excitations and one purely bosonic ones. The boson-fermion interaction thereby is absorbed into inter-dependent coupling constants by renormalizing $g_{\mathbf{k}, \mathbf{q}}$ down to zero via a flow-equation renormalization approach⁴³. At every step of this procedure the renormalized Hamiltonian is projected onto the basic structure given by H_{BFM}^0 plus a renormalization generated

fermion-fermion interactions term⁴⁴

$$H_{BFM}^{F-F} = \frac{1}{N} \sum_{\mathbf{p}, \mathbf{k}, \mathbf{q}} U_{\mathbf{p}, \mathbf{k}, \mathbf{q}}^{F-F} c_{\mathbf{p}\uparrow}^\dagger c_{\mathbf{k}\downarrow}^\dagger c_{\mathbf{q}\downarrow} c_{\mathbf{p}+\mathbf{k}-\mathbf{q}\uparrow}. \quad (4)$$

This is achieved by transforming the Hamiltonian in infinitesimal steps, controlled by a flow parameter ℓ in terms of repeated unitary transformations $H(\ell) = e^{S(\ell)} H e^{-S(\ell)}$, resulting in differential equations $\partial_\ell H(\ell) = [\eta(\ell), H(\ell)]$ with $\eta(\ell) \equiv (\partial_\ell e^{S(\ell)} / \partial_\ell) e^{-S(\ell)}$, determining the flow of the parameters of our system. In its canonical form⁴³, $\eta(\ell) = [H^0(\ell), H(\ell)]$ presents an anti-Hermitian generator. For details of the ensuing coupled non-linear differential equations for the various ℓ dependent parameters $\varepsilon_{\mathbf{k}}(\ell)$, $E_{\mathbf{q}}(\ell)$, $U_{\mathbf{p}, \mathbf{k}, \mathbf{q}}^{F-F}(\ell)$, $g_{\mathbf{k}, \mathbf{q}}(\ell)$, $\mu(\ell)$ we refer the reader to our previous work^{44,45}. The parameters, characterizing H^0 and H^{exch} , evolve as the flow parameter ℓ increases. The renormalization procedure starts with $\ell = 0$, for which they are given by the bare values $\varepsilon_{\mathbf{k}}, E_{\mathbf{q}} = 2\Delta, g_{\mathbf{k}, \mathbf{q}}$ together with $U_{\mathbf{p}, \mathbf{k}, \mathbf{q}}^{F-F} \equiv 0$. The chemical potential $\mu(\ell)$ is chosen at each step of the renormalization flow such as to fix a given total number of fermions and bosons. The flow of these parameters converges for $\ell \rightarrow \infty$ and results in two uncoupled systems: one for the effective fermionic excitations and one for the effective bosonic ones with a fixed point Fermion dispersion $\varepsilon_{\mathbf{k}}^* = \varepsilon_{\mathbf{k}}(\ell \rightarrow \infty)$. For isotropic exchange coupling and fermion dispersion this problem had been studied previously^{37,44,45}, predicting the pseudogap⁴⁶ and damped Bogoliubov modes⁴⁵ in angle resolved photoemission spectra. Both have since been verified experimentally¹.

IV. THE BOSON-FERMION DUALITY.

The anisotropy of the electronic structure of cuprates tracks a change-over from self-trapped (localized) fermions, in form of diffusively propagating bosonic pairs, into itinerant propagating (delocalized) fermions upon going from the anti-nodal to the nodal point on an arc in the Brillouin zone, determined by $\varepsilon_{\mathbf{k}_F}^*(\phi) = \mu$. To illustrate that, we evaluate the single-particle spectral function for wave vectors $\mathbf{k} = |\mathbf{k}|[\sin\phi, \cos\phi]$, orthogonally intersecting this arc at various $\mathbf{k}_F(\phi)$, where the motion of the charge carriers is essentially one dimensional. ϕ denotes the angle of those \mathbf{k} -vectors with respect to the line $[\pi, \pi] - [\pi, 0]$, (see Fig.3).

In order to relate our study to a nearly half filled band situation, characterizing the doped cuprates, we choose $\Delta \simeq 0.75$ (in units of a nominal fermionic band width of $8t$), with the bosonic level lying just barely below the center of the itinerant fermion band such as to reproduce the typical shape of the CuO_2 planar Fermi surface. Our choice of the boson-fermion exchange coupling strength $g = 0.1$, yields a typical onset temperature $T^* = 0.016$ for the pseudogap of roughly a hundred degrees K. For a characteristic temperature of the pseudogap phase

($T = 0.007 < T^*$), it implies a concentration of itinerant fermionic charge carriers $n_F = \sum_{\mathbf{k}\sigma} \langle c_{\mathbf{k}\sigma}^\dagger c_{\mathbf{k}\sigma} \rangle = 0.88$ and that of self-trapped ones bound into fermion pairs, $n_B = \sum_{\mathbf{q}} \langle b_{\mathbf{q}}^\dagger b_{\mathbf{q}} \rangle = 0.075$. This corresponds to a hole doping $n_h = 0.12$, with a total number of carriers of $n_{tot} = n_F + 2n_B = 1.03$. Hole doping redistributes the relative occupation of fermions and bosons which ultimately leads to a shrinking of the arcs (see section V). The charge carriers around the nodal point are primarily given by delocalized fermionic one-particle states, while at the hotspot anti-nodal points they are localized bosonic bound fermion pairs. Yet, as we shall see below, they will become itinerant and eventually condense as the temperature is decreased. The reason for that is that the bare exchange coupling $g_{\mathbf{k}, \mathbf{q}}$ is equal to zero at the nodal point ($\phi = \pi/4$) and increases as one moves to the anti-nodal points ($\phi = 0, \pi/2$), where it reaches its maximal value, equal to g . As a consequence, $\varepsilon_{\mathbf{k}}^*$ remains essentially unrenormalized for \mathbf{k} vectors crossing the arc near the nodal point. Upon approaching the anti-nodal point, on the contrary, $\varepsilon_{\mathbf{k}}^*$ acquires a sharp S-like inflexion at $\mathbf{k}_F(\phi)$, which leads to the appearance of the pseudogap in the single-particle density of states.

Our prime objective in the present study is to disentangle the contributions to the single-particle spectral function coming from the itinerant and from the localized features. The latter arise from single-particles being momentarily trapped in form of localized pairs. The effective fermionic and bosonic excitations are obtained in a renormalization procedure similar to that of the Hamiltonian, but this time by applying it to the fermion and boson operators themselves^{45,47}. The evaluation of the single-particle spectral function

$$A^F(\mathbf{k}, \omega) = -\frac{1}{\pi} \text{Im} \int_0^\beta d\tau G^F(\mathbf{k}, \tau) e^{(\omega+0^+)\tau}$$

$$G_F(\mathbf{k}, \tau) = \langle \langle c_{\mathbf{k}\uparrow}(\tau); c_{\mathbf{k}\downarrow}^\dagger \rangle \rangle_H \quad (5)$$

in a correspondingly renormalized manner is achieved by applying the unitary transformation $e^{S(\ell)}$ to the Green's function itself. It results in

$$\langle \langle c_{\mathbf{k}\sigma}(\tau); c_{\mathbf{k}\sigma}^\dagger(0) \rangle \rangle_H =$$

$$\langle \langle e^{S(\ell)} e^{\tau H(\ell)} c_{\mathbf{k}\sigma} e^{-\tau H(\ell)} e^{-S(\ell)}; e^{S(\ell)} c_{\mathbf{k}\sigma}^\dagger e^{-S(\ell)} \rangle \rangle_{H(\ell)} =$$

$$\langle \langle e^{S(\infty)} e^{\tau H^*} c_{\mathbf{k}\sigma} e^{-\tau H^*} e^{-S(\infty)}; e^{S(\infty)} c_{\mathbf{k}\sigma}^\dagger e^{-S(\infty)} \rangle \rangle_{H^*}, \quad (6)$$

where the trace has to be carried out over the fully renormalized fixed point Hamiltonian H^* . Neglecting the residual interaction $U_{\mathbf{p}, \mathbf{k}, \mathbf{q}}^{F-F}$ between the fermions and restricting ourselves to the pseudogap phase without any long range phase locking, we obtain the following renormalized fermion operators⁴⁷:

$$\begin{bmatrix} c_{-\mathbf{k}, -\sigma}^\dagger(\ell) \\ c_{\mathbf{k}, \sigma}(\ell) \end{bmatrix} = u_{\mathbf{k}}^F(\ell) \begin{bmatrix} c_{-\mathbf{k}, -\sigma}^\dagger \\ c_{\mathbf{k}, \sigma} \end{bmatrix}$$

$$\mp \frac{1}{\sqrt{N}} \sum_{\mathbf{q}} v_{\mathbf{k}, \mathbf{q}}^F(\ell) \begin{bmatrix} b_{\mathbf{q}}^\dagger c_{\mathbf{q}+\mathbf{k}, \sigma} \\ b_{\mathbf{q}} c_{\mathbf{q}-\mathbf{k}, -\sigma}^\dagger \end{bmatrix}, \quad (7)$$

with ℓ dependent parameters $u_{\mathbf{k}}^F(\ell), v_{\mathbf{k}}^F(\ell)$ determined by the flow equations. The single-particle fermionic spectral function resulting from such a procedure

$$A^F(\mathbf{k}, \omega) = |u_{\mathbf{k}}^F(\infty)|^2 \delta(\omega + \mu - \varepsilon_{\mathbf{k}}^*) + \frac{1}{N} \sum_{\mathbf{q} \neq 0} (n_{\mathbf{q}}^B + n_{\mathbf{q}-\mathbf{k}\downarrow}^F) |v_{\mathbf{k},\mathbf{q}}^F(\infty)|^2 \delta(\omega - \mu + \varepsilon_{\mathbf{q}-\mathbf{k}}^* - E_{\mathbf{q}}^*), \quad (8)$$

is illustrated in Fig. 2 for $T = 0.007$ ($< T^* = 0.016$), which lies in the pseudogap phase. We choose a \mathbf{k} traversing the arc in the Brillouin zone at $\mathbf{k}_F(\phi)$, in a characteristic region around $\phi = \phi_c = 15^\circ$, where the T independent gap for $\phi \leq \phi_c$ changes over into a T dependent gap in the single-particle density of states for values of $\phi \geq \phi_c$ (see Fig 3). ϕ_c signals the separation between localized and delocalized, respectively bosonic and fermionic, features in the Brillouin zone.

For \mathbf{k} vectors below $\mathbf{k}_F(\phi)$, $A^F(\mathbf{k}, \omega)$ exhibits (i) low energy ($\leq \mu$) delocalized single-particle excitations (the first term in eq. 8), which follow essentially the dispersion $\varepsilon_{\mathbf{k}}^* \simeq \varepsilon_{\mathbf{k}}$ and (ii) a high energy ($\geq \mu$) broadened upper Bogoliubov like branch. For $k \rightarrow 0$ that latter merges into the time reversed spectrum $-\varepsilon_{\mathbf{k}}$. For wave vectors \mathbf{k} above $\mathbf{k}_F(\phi)$, $A^F(\mathbf{k}, \omega)$ shows simultaneously two features: (i) low frequency diffusively propagating Bogoliubov modes and (ii) high frequency single-particle excitations with a dispersion given by $\varepsilon_{\mathbf{k}}^* \simeq \varepsilon_{\mathbf{k}}$ and moving in a cloud of bosonic two-particle excitations in form of bonding and antibonding states, seen by the wings on either side of the coherent part (the first term in Equ. 8) of those excitations. These low and high frequency excitations for a given wave-vector characterize the low and high frequency response of one and the same phenomenon, with the latter testing the internal degrees of freedom of the collective diffusively propagating Bogoliubov like modes. These internal degrees of freedom are images of localized bonding and anti-bonding states, such as given by the Green's function in the atomic limit ($t, t' = 0$)^{48,49}, $G_{at}^F(i\omega_n) = 1/[G_{at}^F(i\omega_n)^{-1} - \Sigma_{at}^F(i\omega_n)]$ with the selfenergy

$$\Sigma_{at}^F(i\omega_n) = \frac{(1-Z)g^2(i\omega_n + \mu)}{[(i\omega_n + \mu)(i\omega_n - 2\Delta + \mu) - Zg^2]}, \quad (9)$$

which differs qualitatively from any BCS like structure of Cooperons, because taking into account their intrinsic single-particle localized internal degrees of freedom. $Z \simeq 2/[3 + \cosh(g/k_B T)]$ (for our choice of parameters) denotes the spectral weight of non-bonding delocalized charge carriers, described by $G_0^F(i\omega_n) = 1/(i\omega_n - \mu)$.

The pseudogap in the density of states, $\rho(\omega) = (1/N) \sum_{\mathbf{k}} A^F(\mathbf{k}, \omega)$, which opens up at some $T = T^*$ at $\mathbf{k}_F(\phi)$ has a size $\Delta_{pg}(\phi)$. It is determined by the distance between the peaks either side of $\varepsilon_{\mathbf{k}_F(\phi)}^*$, when upon lowering T the deviation from the bare density of state, $\rho^0(\omega) = (1/N) \sum_{\mathbf{k}} \delta(\omega - \varepsilon_{\mathbf{k}})$ becomes noticeable. We take as a criterion a reduction to 90% of $\rho^0(\omega = 0)$. The sharp peak in $A^F(\mathbf{k}_F, \omega)$ in Fig. 2, arising from

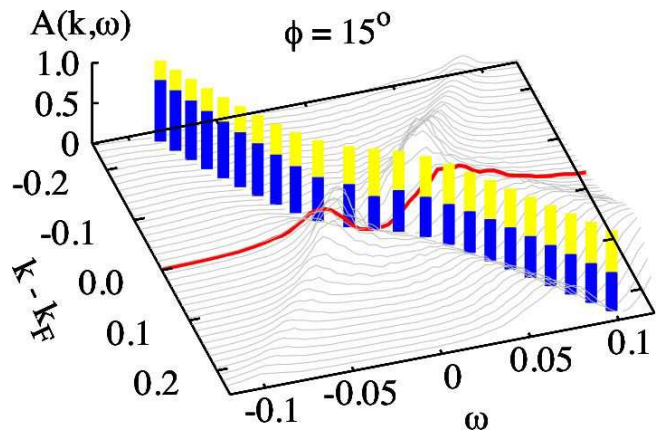


FIG. 2: (Color online) $A(\mathbf{k}, \omega)$ at $T = 0.007$ ($< T^* = 0.016$) as a function of $|\mathbf{k}|$ (in units of the inverse lattice vector) near \mathbf{k}_F (red line), corresponding to $\phi = 15^\circ$, orthogonally crossing the Fermi arc. The spectral weight of the coherent and incoherent contributions are indicated by blue, respectively yellow bars.

the coherent part of this spectrum, is a consequence of having neglected the residual fermion-fermion interaction $U_{\mathbf{p},\mathbf{k},\mathbf{q}}^{F-F}$, eq. 4. The effect of this interaction is to broaden this delta function like peak, as we know from previous studies using different approaches^{50,51}. To describe this effect within the present flow equation approach, requires a fully self-consistent treatment of the diagonal part of the renormalized fermions given by $\sum_{\mathbf{k}\sigma} (\varepsilon_{\mathbf{k}}^* - \mu) c_{\mathbf{k}\sigma}^\dagger c_{\mathbf{k}\sigma}$ and the residual fermion-fermion interaction H_{BFM}^{F-F} - an issue, which will be treated in some future study.

The appearance of the pseudogap is associated with a reduction of the spectral weight of this coherent contribution (given by the height of the blue bars in Fig. 2). We illustrate in Fig. 3 the variation of $\Delta_{pg}(\phi)$ for different T . Close to the anti-nodal point - the localized and bosonic dominated regime - it is relatively T independent. But approaching the nodal point, it abruptly drops to zero, even though $g_{\mathbf{k},\mathbf{q}}$ is still finite. Although reminiscent of BCS like superconducting correlations (without

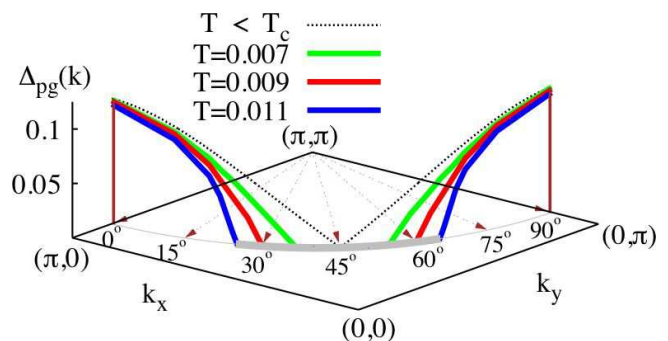


FIG. 3: (Color online) Variation of the pseudogap for different T vectors, orthogonally crossing the arc, given by angles ϕ .

any pseudogap) for $60^\circ \geq \phi \geq 30^\circ$, the momentum dependence of the gap in the superconducting phase is T dependent. This, clearly is not a BCS mean-field type behavior⁵². The reason behind the change-over from an essentially T independent gap for $\phi \leq \phi_c$ and a T dependent gap for $\phi \geq \phi_c$ is the following: As ϕ decreases, the size of the pseudogap increases and at the same time its position in the Brillouin zone at some $\mathbf{k}_F(\phi)$ diminishes until it reaches the bottom of $\varepsilon_{\mathbf{k}}^*$. (see Fig. 2 in Ref. 37). At this point, itinerant fermionic charge carriers disappear in that part for the Brillouin zone, having been converted into bosonic fermion pairs. The accumulation of such bosonic charge carriers near the anti-nodal point is a direct consequence of the anisotropic boson-fermion exchange coupling and d-wave pairing in those cuprates. Since the excitation energies (size of the pseudogap) characterizing such entities are determined by purely local effects, they are relatively temperature as well as doping independent for $\phi \leq \phi_c$. Doping dependent however is the value $\phi = \phi_c$ of the cross-over to itinerant charge carriers, as confirmed in ARPES experiments⁵².

In order to visualize the accumulation of bosonic charge carriers near the anti-nodal points let us investigate how the fermionic charge carriers in the various regions near the arc in the Brillouin zone get converted into diffusively propagating bound pairs of them. To do that we evaluate the renormalized Bose spectral function,

$$A^B(\mathbf{q}, \omega) = -\frac{1}{\pi} \text{Im} \int_0^\beta d\tau G^B(\mathbf{q}, \tau) e^{(\omega + i0^+) \tau}$$

$$G^B(\mathbf{q}, \tau) = \langle \langle b_{\mathbf{q}}(\tau); b_{\mathbf{q}}^\dagger \rangle \rangle_H, \quad (10)$$

for which we had previously derived the corresponding renormalization flow equations⁴⁷. It results in renormalized boson operators

$$b_{\mathbf{q}}(\ell) = u_{\mathbf{q}}^B(\ell) b_{\mathbf{q}} + \frac{1}{\sqrt{N}} \sum_{\mathbf{k}} v_{\mathbf{q}, \mathbf{k}}^B(\ell) c_{\mathbf{k}\downarrow} c_{\mathbf{q}-\mathbf{k}\uparrow}, \quad (11)$$

with $b_{\mathbf{q}}^\dagger(\ell) = (b_{\mathbf{q}}(\ell))^\dagger$, which ultimately leads to the renormalized Boson spectral function given by

$$A^B(\mathbf{q}, \omega) = |u_{\mathbf{q}}^B(\infty)|^2 \delta(\omega - E_{\mathbf{q}}^*) + \frac{1}{N} \sum_{\mathbf{k}} f_{\mathbf{k}, \mathbf{q}-\mathbf{k}} |v_{\mathbf{q}, \mathbf{k}}^B(\infty)|^2 \delta(\omega - \varepsilon_{\mathbf{k}}^* - \varepsilon_{\mathbf{q}-\mathbf{k}}^*). \quad (12)$$

The corresponding number of such bosonic charge carriers is given by $n^B(q_x, q_y) = \int d\omega A^B(\mathbf{q}, \omega) [\exp(\omega/k_B T) - 1]^{-1}$. We plot it for a series of \mathbf{q} vectors in Fig. 4 for $T=0.007$, which sample the anisotropy of the CuO_2 electronic structure, where θ indicates the azimuthal angle in this plane. Notice that along the nodal direction the number of bosons is independent on $|\mathbf{q}|$, because of the absence of any boson-fermion coupling. As one approaches the direction linking the center of the zone with the anti-nodal points, the exchange coupling steadily increases and consequently the intrinsically localized bosons acquire itinerancy and gather in a region

of long wavelength. Those bosons have internal structure of two fermions with opposite momenta centered around $\mathbf{k}_F(\phi)$. In the inset of Fig. 4 we illustrate the total number of such bosons along the various \mathbf{q} vectors and notice the relative increase, respectively decrease compared to their average value 0.075, depending on whether we are sampling the nodal or the anti-nodal directions. The accumulation of fermions getting converted into fermion pairs in certain parts of the Brillouin zone, close the anti-nodal points, has its counter part in the diminishing density of single-particle fermionic excitations in the same regions. We illustrate that in Fig. 5, where we plot the variation of the coherent part of the single-particle dispersion, given by $\varepsilon_{\mathbf{k}}^*$ around $\mathbf{k}_F(\phi)$. We notice that with diminishing ϕ , approaching the anti-nodal points, the corresponding value of $\mathbf{k}_F(\phi)$ diminishes. This announces a shrinking of the Fermi sea, causing an emptying out of single-particle states and consequently an increase of bound fermion pairs. This feature had previously been observed in connection with the transition between the superconducting state of phase correlated bonding pairs and the insulating state of such phase uncorrelated bonding pairs³⁷.

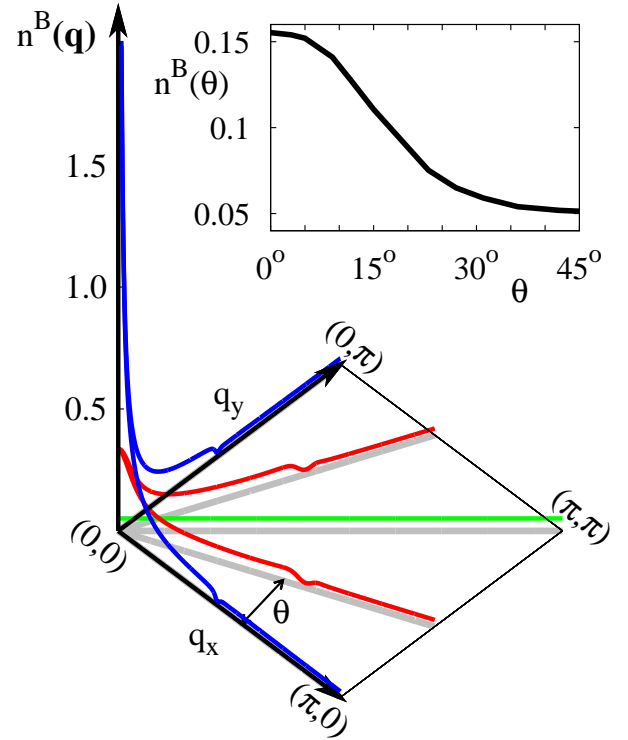


FIG. 4: (Color online) Variation of the number of paired fermions as a function of wavevectors \mathbf{q} along different directions in the Brillouin zone given by the angle θ . The variation of the total number of such pairs is illustrated in the inset.

V. SUMMARY AND OUTLOOK

Our scenario for the cuprate superconductivity is based on resonant pairing, induced by local dynamical lattice instabilities upon hole doping. It makes use of the fact that such systems are prone to a segregation of globally homogeneous crystal structures into small nano-size pairing domains. This breaks locally the translational as well as rotational symmetry by randomly orienting uni-directional Cu-O-Cu molecular bonds in different directions. As a result, the fermionic charge carriers acquire single-particle spectral features which comprise simultaneously: (i) quasi localized states, where they are momentarily trapped in form of bound pairs in polaronic charge fluctuating local domains and (ii) delocalized states on a sublattice in which those polaronic domains are embedded.

Due to the d-wave pairing, which in our case is encoded in the anisotropic Boson-Fermion exchange coupling $g_{\mathbf{k},\mathbf{q}}$, the spectral properties of the single-particle excitations exhibit a pseudogap with the following features: As we move on a constant energy line in the Brillouin zone, corresponding to the chemical potential (where such an arc determines the Fermi surface, whenever it exists), $|g_{\mathbf{k},\mathbf{q}}|$ diminishes as we go from the anti-nodal ($\phi \simeq 0$) to the nodal region ($\phi \simeq \pi/4$). Concomitantly the size of the pseudogap, Δ_{pg} , decreases. For $0 < \phi < \phi_c$, with $\phi_c \simeq 15^\circ$ for our choice of parameters, it remains relatively unaffected by changes in temperature T . On the contrary, for $\phi_c < \phi < \pi/4$, Δ_{pg} becomes strongly T dependent. For low T , it tends to zero gradually as one approaches $\phi = \pi/4$. With increasing T , it tends to zero at increasingly larger values of ϕ , (see Fig.3), as observed

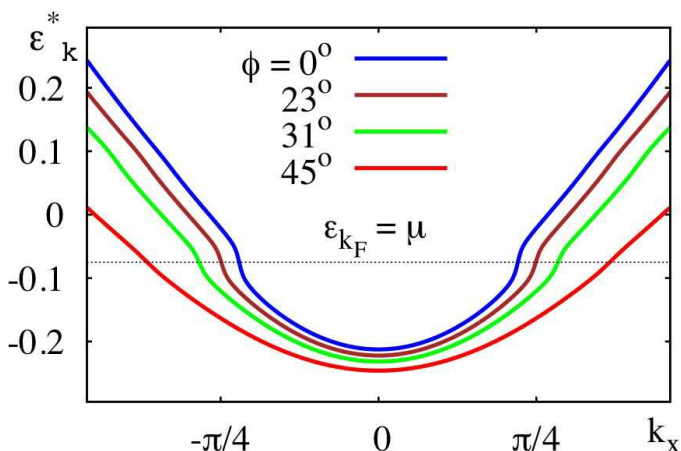


FIG. 5: (Color online) Variation of the renormalized single-particle dispersion for wave-vectors \mathbf{k} orthogonally crossing the arcs along different directions in the Brillouin zone, characterized by the angle $\phi = \arcsin(k_x/|\mathbf{k}|)$. The reduction in the value of $|\mathbf{k}_F(\phi)|$ upon approaching the anti-nodal regime indicates an emptying out of the fermionic single-particle excitations in favor of an increase in their paired states.

experimentally⁶. This suggest that:

(i) the pseudogap in a finite region ($0 < \phi < \phi_c$) around the anti-nodal point is controlled by predominantly local pairing (via intra-*bonding-pair* correlations), which is independent on doping and largely unaffected by superconducting phase fluctuations.

(ii) the pseudogap in a finite region ($\phi_c < \phi < \pi/4$) around the nodal point is controlled by both, local intra-*bonding-pair* as well as non-local superconducting inter-*bonding-pair* correlations, which are sensitive to phase fluctuations and cause the dependence of Δ_{pg} on T as well as on doping.

The diffusively propagating low energy Bogoliubov like excitations around \mathbf{k}_F , which trace out the pseudogap, are a hallmark of the single-particle spectral features of such resonant pairing systems and which exist even near the anti-nodal points. In contrast to a BCS scenario, here, their appearance above T_c does not require a phase coherence of the bosonic bound fermion pairs. Such Bogoliubov like modes nucleate from local intra-*bonding-pair* correlations between pairs of itinerant fermions and localized fermion pairs^{48,49} on local molecular clusters, such as discussed here. They are a signature of a prevailing glassy Bose metallic behavior prone to transit into a superconducting state of phase correlated such bosonic intra-*bonding-pairs*. The momentum dependence of those two-particle excitations, shows a strong tendency toward condensation (see Fig. 4), which tracks the anisotropic behavior of the gap. Provided the Boson-Fermion exchange coupling is not too big, such bosonic pairs forming near the anti-nodal points, will dominate the superconductivity, against a widespread opinion that they should be localized there. For sufficiently large g , they of course will be localized. This is a topic which will require further investigations, dealing with the superconductor to insulator (Bose glass) transition with reduced hole doping. The internal structure of those diffusively propagating Cooperons, consisting of selftrapped fermions, is manifest in their single-particle excitations above the chemical potential. It reflects their atomic localized nature, where two-particle localized bonding and anti-bonding satellites trail the dispersion of their delocalized coherent contributions^{48,49}. The low energy diffusive collective Bogoliubov excitations and the high energy single-particle excitations are two different manifestations of the same entity. Whether there is a sharp border line for the onset of the high energy localized features in the Brillouin zone, as suggested by a so-called doping independent "extinction line"^{6,41}, will have to be checked in future for the present scenario.

Let us conclude this study with some remarks on the kind of doping mechanism we can envisage in the cuprate high T_c compounds. For low hole doping it can be understood in terms of a doped Mott insulator and an antiferromagnetic ground state, transiting into a spin singlet liquid glassy state with increased doping. For the remaining doping regime, approaching the optimal and overdoped regions, it remains largely an open problem

to be resolved. Experimentally one finds a singular universal optimal doping rate $n_h^{opt} = 0.16$ holes/Cu atom, where T_c reaches its maximum together with a maximal volume fraction of the Meissner effect and a Hall number becoming sharply peaked⁵³. In scenarios, like the present one, based on inter-related amplitude and phase fluctuations, optimal doping also characterizes the region where the energies of the superconducting phase stiffness and that of the pairing coincide²⁶. These doping dependent electronic features are accompanied by a reduction of the buckling of the CuO_2 planes¹³, which characterizes the low doped insulating phase. Pressure tuned electronic transitions, testing electronic and lattice features at the same time⁵⁴, point to a critical pressure which can be identified with the critical doping rate n_h^{opt} . The universal value of $n_h^{opt} = 0.16$, occurs for any optimally doped system, whatever the chemical structure of the doping blocks might be. This suggests that, upon approaching optimal doping, the electronic and lattice degrees of freedom must get strongly locked together⁵⁵ and by doing so increase the stability of these intrinsically metastable materials. And indeed, upon trying to force extra holes into such systems by overdoping $n_h > n_h^{opt}$, they segregate into different crystalline phases⁵⁶, with superconducting components composed of underdoped and optimally doped regions. Understanding the doping dependence of the cuprates thus becomes tantamount to understanding the structural stability of those system. It necessarily must involve correlated macroscopic features^{22,23} of charge and lattice deformations, such that precisely at optimal doping they optimally and constructively interfere with each other.

Transposing these experimental facts on the scenario discussed in this paper, the fluctuating local domains in the CuO_2 planes get increasingly coherently locked together as hole doping increases. This results in a decrease of spatial phase fluctuations of the bosonic resonantly bound fermion pairs driven by locally fluctuating lattice structures, while at the same time their conjugate amplitude fluctuations increase. As a consequence T_c increases and T^* decreases. Previous studies^{57,58} on the interplay between amplitude and phase fluctuations bare that out.

According to the presently available experimental facts (Ref. 13,34,35,53-55), the chemical doping mechanism, which imposes itself in the cuprates (following our scenario), converts part of the itinerant electrons into polaronically driven resonating pairs, predominantly in certain regions of the Brillouin zone (see Fig. 4) near the anti-nodal points. It manifests itself in the opening of a pseudogap, which nucleates at the so-called hot-spots, where the local Boson-Fermion exchange coupling g is maximal. The self-regulating redistribution of itinerant charge carriers and bosonic bound pairs of them on the arcs in the Brillouin zone, is an intrinsic rather than an extrinsic⁵⁹ feature of the scenario presented here. It orig-

inates from strong electron-lattice coupling, in a system with a highly anisotropic electronic dispersion and coupling to local lattice modes, evidenced in the anisotropic isotope dependent pseudogap and responsible for the local symmetry breaking of those systems. Given this experimental situation, we conjecture that hole doping primarily will replace the buckled $\text{Cu}^{II}\text{-O-Cu}^{II}$ bonds by unbuckled $\text{Cu}^{III}\text{-O-Cu}^{III}$ ones, whose density n_B will be roughly given by $\frac{1}{2}n_h$, n_h denoting the concentration of chemically doped holes. Doping a single hole into the basic cluster of our segregated CuO_2 planes means a doping rate of $1/8 = 0.125$ per Cu ion. This is very close to the critical doping rate, which changes the insulating glassy phase into the superconducting one. Doping a hole into the trapping centers breaks a $\text{Cu}^{II}\text{-O-Cu}^{II}$ bond. Since this is not compatible with the basic square planar CuO_4 structure in the CuO_2 planes, doping will trigger a charge transfer between the trapping centers and the surrounding four-site rings, either by transferring an electron from the ring to the trapping center and re-establish the stable square planar $\text{Cu}^{II}\text{-O-Cu}^{II}$ bond, or by transferring an electron from that hole doped bond into the ring and leave behind a stable square planar $\text{Cu}^{III}\text{-O-Cu}^{III}$ bond. Both of these processes act together to ensure the overall crystalline stability in systems with intrinsic local dynamically correlated charge-lattice fluctuations and thus result in resonant pairing of the itinerant electrons on the ring. The end-effect of this is a transfer of a fraction n_F^h of the electrons on the ring into the pairing centers, where they form pairs on a finite time scale with a concentration $n_B = \frac{1}{2}n_F^h$. This simultaneously implies a shrinking of the Fermi surface. $n_{tot} = n_F + 2n_B$ in this doping procedure remains unaltered i.e., equal to unity as it is in the undoped case. The effect of hole doping is hence to change the relative concentration of itinerant electrons with respect to the concentration of partly bound pairs of them.

A multitude of different experimental results discussed here have been shown to be compatible with the resonant pairing scenario. Qualitatively different from any BCS pairing scenario, here the itinerant delocalized Bogoliubov excitations coexist with localized single-particle ones which are selftrapped inside of them. Concerning the origin of this resonant pairing in the cuprates, which could be electronic¹⁸, as well as polaronic, the recently observed breakdown of their homogeneous crystal structures into translational/rotational symmetry broken local clusters⁶, gives us confidence that dynamical lattice deformations should play a determinant role in the superconducting state of high T_c compounds.

VI. ACKNOWLEDGEMENT

We thank Juergen Roehler for constructive remarks concerning this work and its presentation.

-
- ¹ A. G. Loeser, Z.-X. Shen, D. S. Dessau, D. S. Marshall, C. H. Park, P. Fournier and A. Kapitulnik *Science* **273**, 325 (1996); H. Ding, T. Yokoya, J. C. Campuzano, T. Takahashi, M. Randeria, M. R. Norman, T. Mochiku, K. Kadowaki and J. Gianpintzakos, *Nature* **382**, 51 (1996); A. Kanigel, U. Chatterjee, M. Randeria, M. R. Norman, G. Koren, K. Kadowaki and J. C. Campuzano *Phys. Rev. Lett.* **101**, 137002 (2008).
- ² Y. Kohsaka, C. Taylor, K. Fujita, A. Schmidt, C. Lupien, T. Hanaguri, M. Azuma, M. Takano, H. Eisaki, H. Takagi, S. Uchida and J. C. Davis, *Science* **315**, 1380 (2007).
- ³ K. K. Gomes, A. N. Pasupathy, A. Pushp, S. Ono, Y. Ando and A. Yazdani, *Nature* **447**, 569 (2007).
- ⁴ K. McElroy, R. W. Simmonds, J. Hoffman, D.-H. Lee, J. Orenstein, H. Eisaki, S. Uchida and J. C. Davis *Nature* **442**, 592 (2003).
- ⁵ T. Valla, A. V. Fedorov, Jinho Lee, J. C. Davis and G. D. Gu, *Science* **314**, 1914 (2006).
- ⁶ Y. Kohsaka, C. Taylor, P. Wahl, A. Schmidt, Jinhwan Lee, K. Fujita, J. W. Alldredge, K. McElroy, Jinho Lee, H. Eisaki, S. Uchida, D.-H. Lee and J. C. Davis, *Nature* **454**, 1072 (2008).
- ⁷ A. W. Sleight, *Physics Today*, **44**(6), 24 (1991).
- ⁸ J. M. Vandenberg and B.T. Matthias, *Science* **198**, 194 (1977).
- ⁹ P. W. Anderson and B. T. Matthias, *Science* **144**, 373 (1964).
- ¹⁰ T. Cuk, F. Baumberger, D. H. Lu, N. Ingle, X. J. Zhou, H. Eisaki, N. Kaneko, Z. Hussain, T. P. Devereaux, N. Nagaosa and Z.-X. Shen, *Phys. Rev. Lett.* **93**, 117003 (2004).
- ¹¹ Jinho Lee, K. Fujita, K. McElroy, J. A. Slezak, M. Wang, Y. Aiura, H. Bando, M. Ishikado, T. Masui, J.-X. Zhu, A. V. Balatski, H. Eisaki, S. Uchida and D. C. Davis, *Nature* **442**, 546 (2006).
- ¹² A. V. Balatsky and J.-X. Zhu, *Phys. Rev. B* **74**, 094517 (2006).
- ¹³ J. Roehler, *Physica C* **408-410**, 458 (2004).
- ¹⁴ D. M. Eagles, *Phys. Status Solidi B* **48**, 407 (1971); K. Cho and Y. J. Toyozawa, *Phys. Soc. Jap.*, **30**, 1555 (1971); H. B. Shore and L. M. Sanders *Phys. Rev. B* **7**, 4537 (1973).
- ¹⁵ S. Ciuchi, M. Capone, E. Cappeluti and G. Sangiovanni, in "Polarons in Bulk materials and systems with reduced dimensionality", Proceedings of International School of Physics "Enrico Fermi", Course CLXI, edited by G. Iadonisi, J. Ranninger and G. de Filippis (IOS Press, Amsterdam, 2006) p 131; A. C. Hewson, *ibid* p. 155 and A. S. Mishchenko, *ibid*. p. 177.
- ¹⁶ J. Ranninger and A. Romano, *Europhys. Lett.* **75**, 461 (2006); J. Ranninger and A. Romano, *Phys. Rev. B* **78**, 054527 (2008).
- ¹⁷ J. E. Hirsch, S. Tang, E. Loh, Jr. and D. J. Scalapino, *Phys. Rev. Lett.* **60**, 1668 (1988).
- ¹⁸ E. Altman and A. Auerbach, *Phys. Rev. B* **65**, 104508 (2002).
- ¹⁹ D. Reznik, L. Pintschovius, M. Ito, S. Iikubo, M. Sato, H. Goka, M. Fujita, K. Yamada, G.D. Gu, and J.M. Tranquada, *Nature* **440**, 1170 (2006).
- ²⁰ P. S. Haefliger, P. Podlesnyak, K. Conder and A. Furrer, *Eur. Phys. Lett.*, **73** 260 (2006).
- ²¹ D. Rubio Temprano, J. Mesot, S. Janssen, K. Conder, A. Furrer, H. Mutka, and K.A. Müller, *Phys. Rev. Lett.* **84**, 1990 (2000).
- ²² R. P. Sharma, T. Venkatesan, Z. H. Zhang, L. R. Liu, R. Chu and W. K. Chu, *Phys. Rev. Lett.* **77**, 4624 (1996); R. P. Sharma, S. B. Ogale, Z. H. Zhang, J. R. Liu, W. K. Chu, Boyed Veal, A. Paulinkas, H. Zheng and T. Venkatesan, *Nature (London)* **404**, 736 (2000).
- ²³ H. A. Mook, M. Mostoller, J. A. Harvey, N. W. Hill, B. C. Chakoumakos and B. C. Sales, *Phys. Rev. Lett.* **65**, 2712 (1990).
- ²⁴ G. Ruani and P. Ricci, *Phys. Rev. B*, **55**, 93 (1997).
- ²⁵ O. V. Misochko, E. Ya. Sherman, N. Umesaki, K. Sakai and S. Nakashima, *Phys. Rev. B*, **59**, 11495 (1999).
- ²⁶ V. J. Emery and S. A. Kivelson, *Nature*, **374**, 434 (1995).
- ²⁷ M. Franz and A. J. Millis, *Phys. Rev. B* **58**, 14572 (1998).
- ²⁸ Y. J. Uemura, G. M. Luke, B. J. Sternlieb, J. H. Brewer, J. F. Carolan, W. N. Hardy, R. Kadono, J. R. Kempton, R. F. Kiefl, S. R. Kreitzman, P. Mulhern, T. M. Riseman, D. Li. Williams, B. X. Yang, S. Uchida, H. Takagi, J. Gopalakrishnan, A. W. Sleight, M. A. Subramanian, C. L. Chien, M. Z. Cieplak, Gang Xiao, V. Y. Lee, B. W. Statt, C. E. Stronach, W. J. Kossler, and X. H. Yu, *Phys. Rev. Lett.* **62**, 2317 (1989).
- ²⁹ M. B. Salamon, Jing Shi, N. Overend and M. A. Howson, *Phys. Rev. B* **47**, 5520 (1993).
- ³⁰ P. Devillard and J. Ranninger, *Phys. Rev. Lett.* **84**, 5200 (2000).
- ³¹ Y. Wang, L. Li and N. P. Ong, *Phys. Rev. B* **73**, 024510 (2006).
- ³² J. Corson, R. Mallozzi, J. Orenstein, J.N. Eckstein, and I. Bozovic, *Nature (London)* **398**, 221 (1999).
- ³³ O. Yuli, I. Asulin, Y. Kalcheim, G. Koren and O. Millo, *Phys. Rev. Lett.* **103**, 197003 (2009).
- ³⁴ Z. Tešanović, *Nature Phys.* **4**, 408 (2008).
- ³⁵ S. Huefner, M. A. Hossain, A. Damascelli and G. Sawatzky, *Rep. Prog. Phys.* **71**, 062501 (2008).
- ³⁶ M. Cuoco and J. Ranninger, *Phys. Rev. B* **74**, 094511 (2006).
- ³⁷ T. Stauber and J. Ranninger, *Phys. Rev. Lett.* **99**, 045301 (2007).
- ³⁸ Z. Tešanović, *Phys. Rev. Lett.* **93**, 217004 (2004).
- ³⁹ T. Pereg-Barnea and M. Franz, *Phys. Rev. B* **74**, 014518 (2006).
- ⁴⁰ J. Ranninger, Proceedings of the International Conference on "Condensed Matter Theories" Quito (2009), *Int. J. Mod. Phys. B* (2010, to be published); *cond-mat:1001.2143v1*.
- ⁴¹ T. Hanaguri, *Nature* **454**, 1062 (2008).
- ⁴² B. Goss-Levi, *Physics Today* **60** (12), 17 (2007).
- ⁴³ F. Wegner, *Ann. Phys. (Leipzig)* **3**, 77 (1994).
- ⁴⁴ T. Domanski and J. Ranninger, *Phys. Rev. B* **63** 134505 (2001).
- ⁴⁵ T. Domanski and J. Ranninger, *Phys. Rev. Lett.* **91**, 255301 (2003).
- ⁴⁶ J. Ranninger, J. M. Robin and M. Eschrig, *Phys. Rev. Lett.* **74**, 4027 (1995).
- ⁴⁷ T. Domanski and J. Ranninger, *Phys. Rev. B*, **70**, 184503 (2004).
- ⁴⁸ T. Domanski, J. Ranninger and J. M. Robin, *Solid State Commun.* **105**, 473 (1998).
- ⁴⁹ T. Domanski, *Eur. Phys. J. B* **33**, 41 (2003).
- ⁵⁰ J. Ranninger and J. M. Robin, *Solid State Commun.* **96**,

- 559 (1996).
- ⁵¹ J. M. Robin, A. Romano and J. Ranninger, Phys. Rev. Lett. **81**, 2755 (1998).
- ⁵² W. S. Lee, I. M. Vishik, K Tanaka, D. H. Lu, T. Sasagawa, N. Nagaosa, T. P. Devereaux, Z. Hussain and Z.-X. Shen, Nature **450**, 81 (2007).
- ⁵³ F. F. Balakirev, J. B. Betts, B. Jonathan, A. Migliori, S Ono, Y. Ando and G. S. Boebinger, Nature **424**, 912 (2003).
- ⁵⁴ T. Cuk, V. Struzhkin, T. P. Devereaux, A. F. Goncharov, C. A. Kendziora, H. Eisaki, H.-K. Mao and Z.-X. Shen, Phys. Rev. Lett. **100**, 217003 (2008).
- ⁵⁵ J. Röhler, Proc. Int. Conf. "Materials and Mechanisms of Superconductivity", Tokyo (2009, to be published), cond.mat/0909.1702.
- ⁵⁶ V. P. Martovitsky, A. Krapf and L. Dudy, JETP Lett. **85**, 292 (2007).
- ⁵⁷ J. Ranninger and L. Tripodi, Phys. Rev. B **67**, 174521 (2003).
- ⁵⁸ M. Cuoco and J. Ranninger, Phys. Rev. B **70**, 104509 (2004).
- ⁵⁹ A. Perali, C. Castellani, C. Di Castro, M. Grilli, E. Piegari and A. A. Varlamov, Phys. Rev. B **62**, R9295 (2000).